

Cutaneous Imaging Technologies in Acute Burn and Chronic Wound Care

Chandan K. Sen, PhD
Subhadip Ghatak, PhD
Surya C. Gnyawali, PhD
Sashwati Roy, PhD
Gayle M. Gordillo, MD

Columbus, Ohio



Background: Wound assessment relies on visual evaluation by physicians. Such assessment is largely subjective and presents the opportunity to explore the use of emergent technologies.

Methods: Emergent and powerful noninvasive imaging technologies applicable to assess burn and chronic wounds are reviewed.

Results: The need to estimate wound depth is critical in both chronic wound and burn injury settings. Harmonic ultrasound technology is powerful to study wound depth. It addresses the limitations of optical imaging with limited depth of penetration. What if a wound appears epithelialized by visual inspection, which shows no discharge yet is covered by repaired skin that lacks barrier function? In this case although the wound is closed as defined by current standards, it remains functionally open, presenting the risk of infection and other postclosure complications. Thus, assessment of skin barrier function is valuable in the context of assessing wound closure. Options for the study of tissue vascularization are many. If noncontact and noninvasive criteria are of importance, laser speckle imaging is powerful. Fluorescence imaging is standard in several clinical settings and is likely to serve the wound clinics well as long as indocyanine green injection is not of concern. A major advantage of harmonic ultrasound imaging of wound depth is that the same system is capable of providing information on blood flow dynamics in arterial perforators.

Conclusion: With many productive imaging platforms to choose from, wound care is about to be transformed by technology that would help assess wound severity. (*Plast. Reconstr. Surg.* 138: 119S, 2016.)

In current clinical practice, assessment of wounds mostly relies on visual evaluation by physicians and clinical staff.¹ As a result, the assessment is largely subjective and presents a major opportunity to explore the use of emergent technologies. Visual evaluation of wounds, the current gold standard, has served us well but is clearly not the future of wound care. Key limitations include heavy reliance of experience and subjective variations. Current imaging modalities offer a more in-depth assessment of the wound bed and its surroundings. The ability to obtain 3-dimensional (3D) visualization of the structure as well as function of the wound bed provides information of significant clinical relevance. Most of these

technologies, in their initial stages, require a level of technical expertise that may not be readily available in the wound clinics. However, a number of such technologies have advanced to a state of simplicity that they are being presented as turn-key solutions for clinical applications. It is important to recognize here that as more such platforms enter the clinic, there will be issues related to the interface between technology and clinical staff. Indeed, there will be a burden to train and adjust

Disclosure: *The authors have no financial interest in any of the products, devices, or drugs mentioned in this article.*

Supplemental digital content is available for this article. Direct URL citations appear in the text; simply type the URL address into any Web browser to access this content. Clickable links to the material are provided in the HTML text of this article on the *Journal's* Web site (www.PRSJournal.com).

From the Center for Regenerative Medicine & Cell-Based Therapies, Department of Surgery, Davis Heart and Lung Research Institute, The Ohio State University Wexner Medical Center.

Received for publication February 16, 2016; accepted June 13, 2016.

Copyright © 2016 by the American Society of Plastic Surgeons

DOI: 10.1097/PRS.0000000000002654

such measurements into the clinical workflow routine. It is therefore understandable that introduction of such innovation into the clinical practice environment will frequently encounter resistance as it is likely to initially slow down operations and place additional demands on staff.

In this brief review article, it is our goal to uphold the power of imaging in the wound clinic. On one hand, these platforms will introduce a more objective approach to wound care. On the other hand, they are likely to generate novel observations that would question common practices and even introduce a paradigm shift in wound care research. Here, we discuss developments in noninvasive cutaneous imaging platforms that are likely to be of impact in clinical care. This study is intended to be of value to a clinical audience who are not imaging experts, yet would like to consider options in applying emergent technology to clinical care and research.

WOUND DIMENSION AND CLOSURE

Ideally, assessment of cutaneous wound should include length, breadth, and depth measurements. Depending on the location and variation in wound contours, linear measurements may not be reliable. In case of acute burn injury, burn depth assessment is important in determining the strategy for care.² Furthermore, changes in the depth of burn injury over time are an important predictor of burn conversion and may thus inform clinical care plan. Indeterminate depth burns are commonly encountered challenges for burn surgeons, and in our burn center it is estimated that 75% of indeterminate depth burns are ultimately found to be full-thickness injury. Current clinical practice relies on waiting and visual assessment for the burn to declare before any decision to excise and graft is taken.³ It is estimated that in a clinical care setting, only 64% to 76% of cases benefit from reliable visual inspection.⁴ The current gold standard of accurate assessment of burn depth relies on invasive histological approaches for which tissue biopsies must be obtained.^{5,6} Importantly, such biopsy may not represent the complex heterogeneous properties of the much larger wound. Excessive biopsies of the wound involve burdening the patient,⁷ additional trauma, and pose risks that may complicate the healing process.^{5,6} Three-dimensional assessment of the spatiotemporal changes in wounds, both acute and chronic, represents a compelling clinical need and can be met by a number of emergent technologies. Those that are simple in approach and

are likely to be friendly to the clinical end user are discussed below.

ASSESSMENT OF WOUND DIMENSION

Optical Imaging

Wound area measurement is commonly used to assess wound closure over time. Accuracy and reproducibility of this manual process are low.⁸ Advanced solutions are therefore being provided by platforms where high-resolution digital photography, widely supported by smart phones, is supported by advanced software.⁹ Such approaches continue to be confounded by factors such as variable lighting conditions, distance to the objects, and quality of images that are often not tightly controlled in a clinical care environment. Current smart phones, supported by high-resolution camera, play a major role in the assessment of wound size and documentation. Professional grade performance of the camera is further enhanced by apps developed on Java language and OpenCV library platforms. These apps are therefore readily compatible with a wide array of mobile operating systems (i.e., Android and iOS operating systems). Various user friendly apps are commercially available⁹ for use by wound care clinical staff. If used appropriately, digital photographs may be corrected for attributes such as brightness and shot angle. Numerous commercially available apps include algorithm designed to automatically calculate wound area based on image segmentation and thresholding.^{9,10} Other convenient features such as automatic calculation of change in wound size compared with the last visit are helpful in the process of clinical decision. Based on appearance, images can be recognized, say well-perfused versus necrotic tissue.^{11,12}

As 3D photography using smart phone platforms is becoming common, a few wound imaging products in the market such as E-Kare and Silhouette offer the opportunity for 3D photography of wounds.¹³ Although the claim is that these technologies can address the important issue of wound depth, it is important to acknowledge their limitations. First, the field of view being limited, these platforms may not be best suited for large burns. For such applications, it is important that the system allows the acquisition of multiple digital images, which then would seamlessly integrate into one large image presenting the clinician with a simplified solution minimizing disruption of the clinical work flow. The proposed solution would also be helpful to address body contours where photographs may be acquired at different planes,

yet the software algorithm would include stereo-photogrammetry¹⁴ such that the physician may visualize a flat image of the large wound across different planes of the body. Second, some of the above-mentioned platforms include a digital camera equipped with lasers.¹⁵ The advantage is that the laser tracks are automatically adjusted for camera distance, angle, and for curvature of the skin surface. The disadvantage, however, is that the laser has weak penetration power of 1 to 2 mm, which is reasonable to estimate body contour but not effective in the assessment of deep wounds. Therefore, current technologies available to assess wound depth largely rely on photography. Therefore, these technologies cannot see through a scab or other elements obstructing the line of vision. Measuring the true depth of a wound will require a noninvasive and safe technology platform that can image inches beyond what meets the eye. Ultrasound imaging is well suited for that purpose.¹⁶

Harmonic Ultrasound Imaging

Four decades ago, ultrasound was used to measure wound depth using pulse-echo mode.¹⁷ Ultrasonic techniques quantify physical parameters of biological tissue through measurements of acoustic propagation properties such as velocity, attenuation, absorption, and scattering.¹⁸ Ultrasound imaging utilizes high-frequency sound waves to generate images of the skin tissue via a pulse-echo sequence.⁷ Visualization of 3D structures up to a depth of several inches is therefore possible making ultrasound imaging a powerful tool to study full-thickness wounds. Pulses generated by ultrasound transducer pass through tissue and reflect back producing echoes. A B-mode image is generated by the echoes of reflected and scattered ultrasound waves from tissue boundaries and within tissues. Brightness of the B-mode image is a manifestation of the amplitude of the echo.¹⁹ Noise artifacts and clutter representing undesirable echoes from tissue interfaces may be addressed by the use of harmonics, which markedly improves image quality (Fig. 1). This is possible because limiting the imaging to the harmonic range eliminates much of the near-field artifacts associated with typical ultrasound imaging.

Elastography is a dynamic technique that uses ultrasound to noninvasively assess the mechanical stiffness of tissue by measuring tissue distortion in response to external stretch.^{20,21} A topical transducer applies mechanical stress on the tissue by alternative compression and decompression of the skin, and this stress, measured as axial

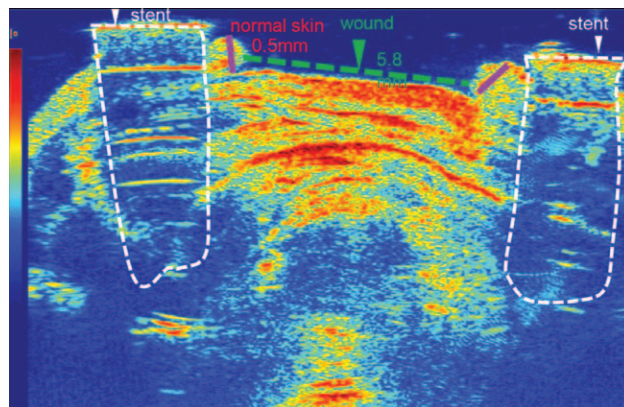


Fig. 1. Ultrasound imaging of wounds. The noble application of the B-mode imaging of ultrasound is that it enables the non-invasive depth and size calculation accurately. Image shows a mouse wound created with a 6-mm punch biopsy on the dorsal skin and was sutured by a 10-mm circular silicon stent. The measurements of wound depth (*purple line*) and wound size (*green dashed line*) are shown. The areas marked with white dotted lines are regions below the silicon stent showing the restriction in transmitting the ultrasound waves into the tissue. A tissue bulge can be seen at the wound site, which is because of the pressure in the absence of skin. B-mode image was color-coded using Matlab program to distinguish the areas of interest clearly.

displacement of tissue, is visualized as an elastogram. The color-coded elastogram shows soft tissue with high strain in red. Intermediate-stiffness tissue with equal strain is seen in green, and hard tissue with negligible strain is shown in blue. Such data can be semiquantitated using a visual scoring system based on the colors or using strain-ratio measurements usually provided in the elastography software.²² Harmonic ultrasonic techniques are powerful for the analysis of skin wounds in particular. Because of the low depth of penetration required, lower frequencies can be used, permitting higher spatial resolution of the sample being analyzed. High spatial resolution enables the visualization of the epidermis, dermis, and subcutaneous fat and the muscle layer. [See Figure, Supplemental Digital Content 1, which shows tissue elastography enabled visualization of the existing and nascent tissue color-coded for their biomechanical properties. Noblus ultrasound system (Hitachi-Aloka Medical, Ltd., Wallingford, Conn.) was used in this imaging. Doppler tissue elastography imaging feature of this system uses the stretching of the tissue when the probe touched the skin and measures the stiffness based on the tissue displacement. A, H&E-stained section of pig skin. B, Tissue stiffness was measured. Skin adipose and muscle can be identified based on the color code. The color-coded scale bar represents the degree of tissue hardness. C,

Representative images of formalin-fixed paraffin-embedded biopsy tissue sections (5 μ m) of normal and wounded skin (day 42) that were stained using Masson's trichrome method. Scale bar = 4 mm. Skin hardness and elasticity of the wound were mapped over time as the wound heals,⁷ <http://links.lww.com/PRS/B811>.] Color-coded elastography is effective in visualizing wound epithelialization where nascent tissue is typically seen in green (Fig. 2). In burn wounds, harmonic ultrasound imaging is capable of visualizing burn thickness (Fig. 2) and occlusion of vascular perforators (Fig. 3). Importantly, it may be utilized to monitor the progression of burn conversion to full thickness informing the clinical care plan. Harmonic ultrasound may cover large areas of injury, and is rapid and noninvasive. In addition, the same system may be used to study wound perfusion as addressed below.⁷

ASSESSMENT OF FUNCTIONAL WOUND CLOSURE

Clinically, wound closure is defined by skin reepithelialization without drainage or dressing requirements confirmed at 2 consecutive study visits 2 weeks apart.²³ Such definition relies on visual assessment of the wound and has been called to question in light of a recent publication demonstrating that under certain conditions the repaired skin may not possess barrier function.²⁴ In other words, it is possible that a wound may be covered with epithelium, but that the repaired skin is functionally deficient.²⁴ Thus, although such wound is physically closed, it is functionally open. Such functional deficit of the skin will allow entry of microorganisms and aeroallergens²⁵ and may result in postclosure wound complications such as recurrence and dehiscence. In patients

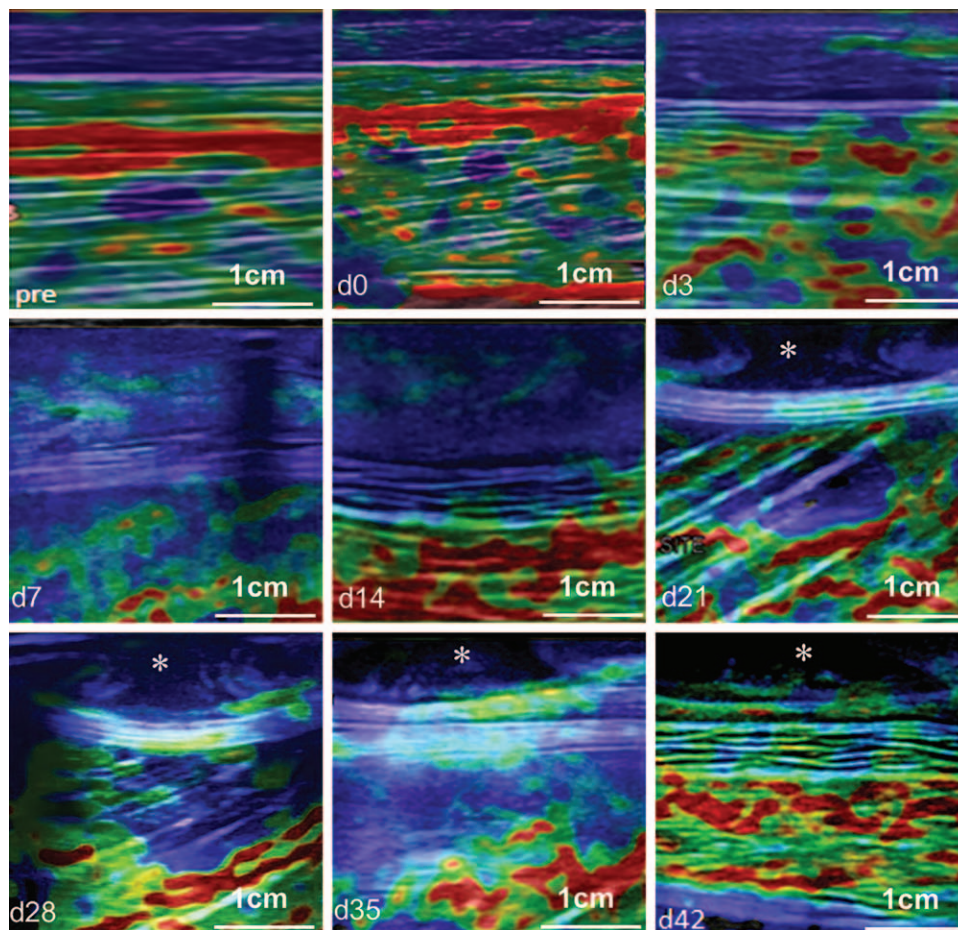


Fig. 2. Tissue elastography enabled visualization of the existing and nascent tissue color-coded for their biomechanical properties. Nobulus ultrasound system (Hitachi-Aloka Medical Inc., Japan) was used in this imaging. Doppler tissue elastography imaging feature of this system uses the stretching of the tissue when the probe touched the skin and measures the stiffness based on the tissue displacement. Color maps of the elasticity of the burn wound in pig tissue over time. Asterisks (d21–d42 images) mark the presence of cavitation area.⁷

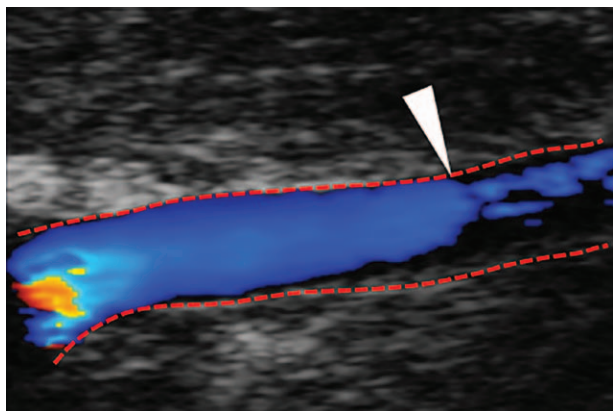


Fig. 3. Ultrasound imaging of the skin vasculature. Doppler ultrasound protocol in artery showing thrombosis as indicated by arrow. Vevo2100 ultrasound imaging system (Visualsonics, Toronto, Canada) with frequency ultrasound linear array probe of frequency 40 MHz was used for image acquisition.

with wounds involving large total body surface area, commonly seen in burn injury, large area of dysfunctional skin may cause systemic complications.²⁵ Skin barrier function is measured by transepidermal water loss.^{24,26–30} Biofilm-infected wounds may not show any difference in the rate of wound closure, but the repaired skin is functionally compromised displaying high transepidermal water loss (TEWL_{hi}).²⁴ To assess functional wound closure, measurement of wound dimension as addressed above should be complemented with the assessment of transepidermal water loss.

ASSESSMENT OF WOUND PERFUSION

In adult skin, the process of neovascularization remains dormant while retaining the ability to initiate inducible angiogenesis, especially in response to injury.³¹ Under physiological conditions, the process of angiogenesis is tightly regulated. Although disruption of the vasculature caused by injury induces angiogenic processes, completion of tissue repair is associated with regression of the excessive vasculature that was necessary to support the hypermetabolic healing tissue.³² In response to wounding, the production of new blood vessels from the preexisting vessels is accompanied by an increase in vascular permeability.^{33,34} At the wound bed, the newly formed blood vessels play a critical role in providing nutrients and oxygen to the granulation tissue.³⁵ Wound revascularization may be impaired by local as well as systemic factors. In acute wounds such as burn injury in an otherwise healthy person, factors such as infection may limit angiogenesis.³⁶ This often leads to graft loss in case of full-thickness burn wound.

Tissue oxygen saturation is a surrogate marker of wound perfusion.³⁷ Ankle brachial index and transcutaneous oxygen measurement are the two clinically used methods for measuring vascular supply to the wound tissue.^{38,39} However, both these methods provide point measurement and are thus not suitable to address the perfusion status over the entire wound area. Current clinically applicable imaging platforms applicable for the study of wound perfusion are discussed below.

Hyperspectral Imaging of Partial Oxygen Saturation

Hyperspectral imaging, also known as the imaging spectrometer, is an advanced form of spectroscopy that provides a 2D tissue oxygenation map using multiple wavelengths of light varying from 410 to 950 nm.⁴⁰ This technology is versatile and has many possible biomedical and even military applications.^{40,41} The unique spectral properties of oxy- and deoxy-Hb provide the basis of hyperspectral imaging of tissue oxygen saturation.⁴² Unique spectral signatures of oxygenated red blood cells (RBCs with oxyhemoglobin) and deoxygenated RBCs (RBCs with deoxyhemoglobin) result in a spectral shift as the oxygenation of the tissue changes. Such spectral shift may be rapidly and highly sensitively detected.^{43,44} Data obtained from the wound tissue are compared with standardized data for these molecules, resulting in a color-coded image. A color bar legend helps understand the levels of wound tissue oxygenation (Fig. 4). A major advantage of this technique is flexibility in scaling the region of interest (ROI) using a tiling approach. However, skin color, blood concentration, adipose content, and ambient illumination may introduce significant variability.⁴⁵ Clinically, the hyperspectral imaging has been used to study skin microcirculation and muscle metabolism of the diabetic foot.⁴⁴ Technically, the hyperspectral imaging platform is fraught with 3 major challenges.⁴⁰ First, because the hyperspectral imaging datasets are large, they are not compatible with video streaming of real-time acquisition. Because higher spectral and spatial resolution and a larger database of tissue spectra provide more spatial and spectral information and may potentially capture more subtle spectral and spatial variations of different tissue types, compression of data set is not simple. Second, hyperspectral imaging requires rapid computational processing of large datasets. Such complexity is a barrier to producing low-cost end-user-friendly devices. The third challenge is to create a spectral database for molecular biomarkers and different tissue types.

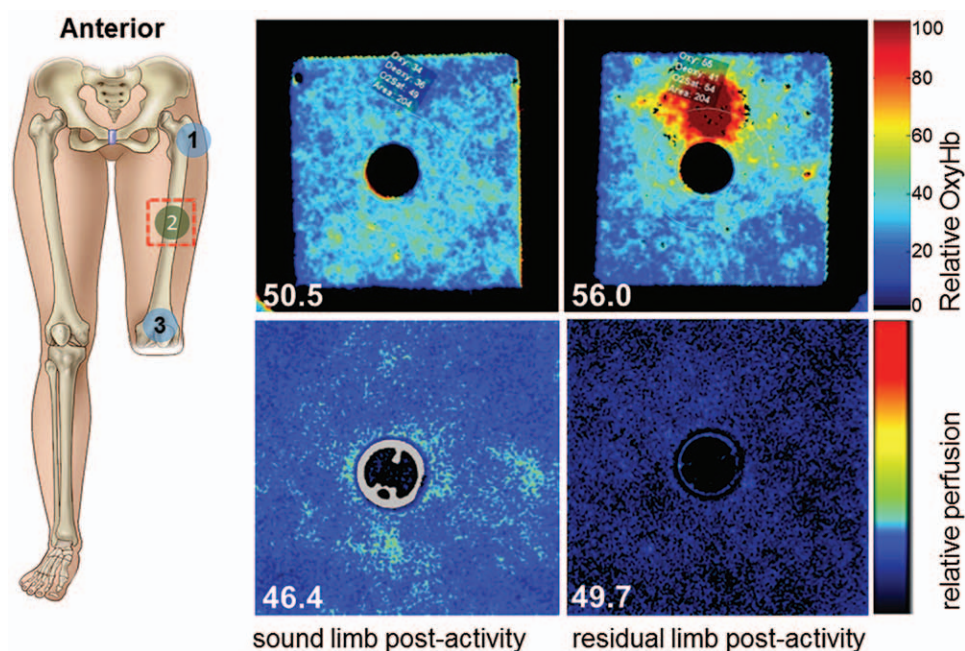


Fig. 4. In persons with leg amputation, the prosthetic limb attachment causes significant pressure at the site of attachment, resulting in altered skin homeostasis in the residual limb. Hyperspectral imaging and LSI were collected from areas of high and low stress within the prosthetic socket on above the knee patients during pre- and postactivity. (Left) The numbers (1, 2, and 3) indicate the order in which the measurements are taken and the number designation for each region (right, above) Oxy-hemoglobin (OxyHb) maps were acquired using hyperspectral imaging system (Hypermed, Inc., Burlington, Mass.) from above-knee-matched ROI (red-dotted box in left panel; number 2 position) in sound and residual limb at rest before liner/socket donning (preactivity) and postactivity. The color-coded maps show variation in tissue oxygen saturation blue as low oxygenated and red as highly oxygen saturated tissue, as shown in the color bar. (Right, below) Laser speckle perfusion images of the same ROI are shown in right, above panel. The numbers in the right panels indicate the oxygen saturation and perfusion values.

Fluorescent Vascular Angiography

The fluorescent dye indocyanine green (ICG) is common used to visualize tissue perfusion during surgery.⁴⁶ Using this approach, surgeons may visually assess and objectively analyze the quality of blood flow in real time intraoperatively.⁴⁶ This technology is now available for the study of wound perfusion.⁴⁶ This platform has several practical advantages, including a turn-key device that is friendly for use by clinical staff.⁴⁷ ICG binds to the lipids of lipoprotein complexes, resulting in more intense fluorescence than ICG bound to, for example, free cholesterol.⁴⁷ The absorption spectrum of ICG lies within the “optical window” of the skin at 600 to 900 nm. Light excited near the infrared range (760–805 nm) is absorbed with fluorescence emission around 835 to 845 nm. This allows tissue penetration up to 10 mm in depth, capturing the vasculature in the deep dermal plexus and subcutaneous fat without the risk for damage to the tissue. Coupling of solid-state

illumination with high-resolution, real-time imaging using sophisticated camera technology produces clinically relevant images of blood flow in vessels and microvessels. ICG fluorescence imaging may also indirectly estimate burn depth.^{48,49}

Some disadvantages of ICG fluorescence imaging include the injection of ICG dye, which makes the procedure invasive.⁵⁰ Although toxicity of ICG is classified as low, it is not without risks during pregnancy. ICG is held to be of minor toxicity. In extreme rare cases, slight side effects of ICG have been reported in humans.⁵¹ In rare cases, effects such as anaphylactic shock, hypotension, tachycardia, dyspnea, and urticaria have been noted. Apart from these adverse biological effects in patients, there can be significant variations in fluorescence due to pulsatile flow, recirculation of dye, and injection artifacts. Hyperfluorescence is usually attributed to abnormal blood vessels with leakage or pooling of dye. Hypofluorescence may also occur due to abnormal vascular filling

as well.⁵² Noninvasive imaging of perfusion without the need for any injection may be achieved by laser speckle imaging (LSI).

LSI of Microvessels

Laser speckle contrast imaging or LSI uses a 785-nm laser to illuminate the wound tissue. The area is marked by another 650-nm laser. Both lasers are safe to work without eye protection. When the ROI is illuminated, the backscattered light forms a random interference pattern consisting of light and dark areas. This constitutes speckle pattern.⁵³ If the illuminated object is static, the speckle pattern is stationary. In case of an object in motion, such as RBCs in a tissue, the speckle pattern will change over time. Depending on the degree of movement, the level of blurring will differ. The more movement, the more blurred will be the corresponding speckle pattern. The level of blurring is quantified by the speckle contrast, creating a speckle pattern to visualize tissue microcirculation in real time by an advanced CCD camera. The camera records the changes in the speckle pattern at a speed of up to 100 images per second and up to 1388×1038 pixels per image. By analyzing the fluctuations in speckle contrast, blurred microvessels are color-coded to generate perfusion maps of the tissue. This system has a precision of $\pm 4\%$ (motility standard) and a perfusion unit of ± 3 (zero perfusion). Blood perfusion is expressed as arbitrary perfusion units. LSI can be performed at standard resolution (for large measurement areas up to 24×24 cm, with a flexible working distance of 10–40 cm) or at high resolution (for small measurement areas up to 0.2×0.27 cm, with a fixed working distance of 10 cm). The high-resolution LSI visualizes the details of $20 \mu\text{m}/\text{pixel}$ (Fig. 5).

Majority of complications in burn injury and chronic wounds, such as tissue necrosis or endothelial and neurovascular function, can be traced back to failed or poor perfusion at the microcirculatory level.⁵⁴ Such alterations in tissue perfusion may be rapidly detected using LSI. Noncontact scan of large areas of almost 10×10 in makes LSI an attractive option for clinical use. A key limitation of LSI is its superficial depth of scan (0.3 mm). As long as the perfusion of an exposed tissue such as skin is of interest, LSI is powerful (Fig. 6). [See **Figure, Supplemental Digital Content 2**, which shows that Laser speckle perfusion imaging shows dynamic changes in wound-site blood flow over time in pigs. Mean perfusion at the wound edge (A) and wound bed (B) from all the time points are shown in the line graph. Data represent mean \pm SD (scale bar = 1 cm) (n = 3 pigs),⁷ <http://links.lww.com/PRS/B812>.] For the study of blood flow dynamics in deeper-lying gated blood vessels, Doppler ultrasound imaging is powerful.⁷

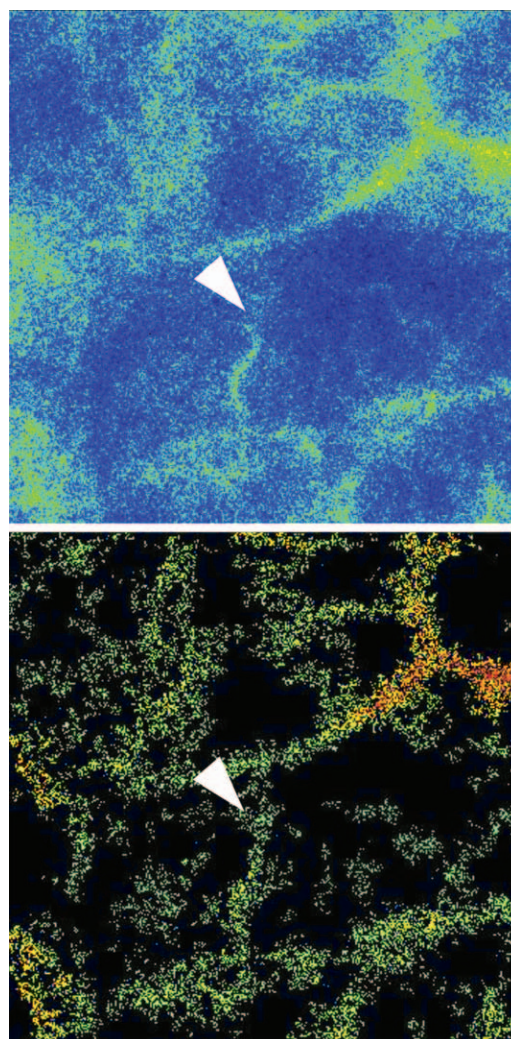


Fig. 5. High-resolution laser speckle contrast analysis on human skin. (Above) Perfusion recordings were performed using a high-resolution ($20 \mu\text{m}$) laser speckle camera (Perimed Inc., Jarfalla, Sweden), and color-coded perfusion map was obtained. After the completion of perfusion recordings, average perfusion was calculated using PimSoft v1.4 software. (Below) The raw perfusion data were then converted to binary raw data videos, and postprocessing was performed using software developed on MATLAB-based platform to visualize the microvasculature. Restricted perfusion is indicated by the white arrows. All human studies were approved by The Ohio State University's Institutional Review Board. Declaration of Helsinki protocols was followed and patients gave their written informed consent.

[See **Figure, Supplemental Digital Content 2**, which shows that Laser speckle perfusion imaging shows dynamic changes in wound-site blood flow over time in pigs. Mean perfusion at the wound edge (A) and wound bed (B) from all the time points are shown in the line graph. Data represent mean \pm SD (scale bar = 1 cm) (n = 3 pigs),⁷ <http://links.lww.com/PRS/B812>.] For the study of blood flow dynamics in deeper-lying gated blood vessels, Doppler ultrasound imaging is powerful.⁷

Ultrasound Doppler Imaging

The same device that provides B-mode harmonic ultrasound imaging of wound depth (discussed in Harmonic Ultrasound Imaging section)

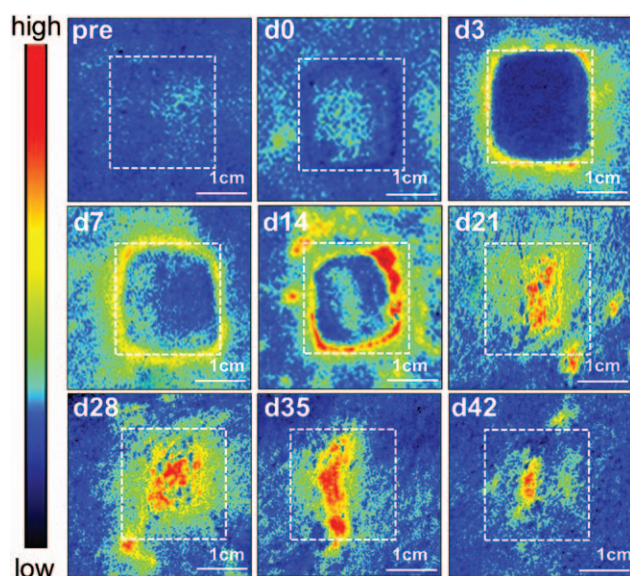


Fig. 6. Laser speckle perfusion imaging shows dynamic changes in wound-site blood flow over time in pigs. Perfusion was visualized as a 2D color-coded map of blood flow (red = high; blue = low). Perfusion maps were acquired for all time points. A dashed line box representing the original wound size (1" × 1") was drawn on perfusion images to show changes in perfusion and wound size over time ($n = 3$ pigs).⁷

is capable of performing dual function by providing the capability of ultrasound Doppler imaging.⁷ B-mode ultrasound imaging works within a frequency range of 20 to 200 MHz. In the case of full-thickness deep wounds or large burns where the superficial microvascular network is completely devastated, the wound tissue relies on perforator arteries for reperfusion of the site of injury.⁵⁵ On one hand, at the surface microenvironmental cues induce the generation of angiogenic factors and proliferation of vascular cells. During the tissue repair process, this angiogenic cascade unfolds such that following resolution of inflammation a nascent microvascular network is reestablished waiting to be perfused by blood supply from one or more intact perforator arteries supplying the site of injury.⁵⁵ As such artery approaches the site of injury, it plumbs the nascent microvascular network, causing blood to flow through the new microvessels.⁵⁵ This flow provides signals from vascular maturation toward sustained patency.⁵⁵ Thus, hemodynamics in the perforator arteries represent a critical contributor to wound perfusion. The blood flow in these perforator arteries may be gated and all aspects of hemodynamics measured using Doppler ultrasound imaging (Fig. 7). [See Figure, Supplemental Digital Content 3, which shows that ultrasound measurement

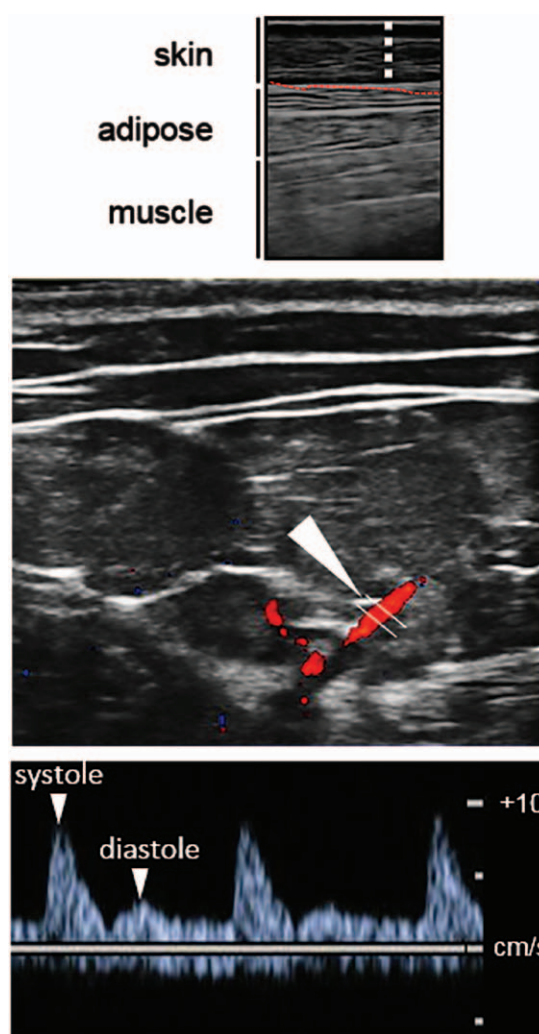


Fig. 7. Ultrasound measurement of pulse pressure indicates enhanced blood flow via feeder vessels supplying the edge of the wound. (Above) Noblus ultrasound system (Hitachi-Aloka Medical Inc., Japan) was used in this imaging skin. (Center) Tissue Doppler color flow imaging feature of this system uses the Doppler principle in which the sound reflects from the pulsating blood particles and the signal is color-coded to red (flow toward probe). This technique is capable of detecting arteries and measuring maximum flow rate in the skin and wound regions. The color-coded images are overlaid on B-mode. Feeder vessels were defined based on the depth of the detected vessels (up to 12 mm deep from the skin surface with the consideration that deeper vessels may not represent the vessel supplying the wound site) and size of vessel detected (using measurement tools in the Hitachi software, vessel size was measured and size-matched vessels were used for flow measurement). Blood flow was performed as indicated by arrow. Gating the blood vessel provided the blood flow velocity profiles as shown below. (Below) Velocity profile images of arterial wound-edge blood flow as measured by pulse wave Doppler flow are shown. Profiles of diastole (peaks) and systole (troughs) are indicated by arrows. From the pulsation caused by systole and diastole of the heart beat, pulse pressure can be calculated using Bernoulli equation.⁷

of pulse pressure indicates enhanced blood flow via feeder vessels supplying the edge of the wound. (A) Velocity profile images of arterial wound-edge blood flow as measured by pulse wave Doppler flow show changes in velocity profile over time. (B) Flow velocities measured using the caliper feature of the software (cm/s) were plotted over time in the graph ($n = 3$ pigs). (C) Mean arterial pulse pressure values (mm Hg) of vessels feeding the wound area were calculated using Bernoulli's modified hemodynamics equation and represented graphically ($n = 3$ pigs). Data represent mean \pm SD,⁷ <http://links.lww.com/PRS/B813>.] Using a linear array probe with a frequency range of 3 to 18 MHz, live imaging of wound tissue and gated flow measurements in perforator arteries can be accomplished within 15 minutes. Typically, depending on the scenario, the wound may be covered by Tegaderm (D-41453; 3M Health Care, Neuss, Germany). Ultrasound coupling gel is applied on the Tegaderm followed by scanning of the wound tissue.⁵⁶ The same scan provides information on wound depth using B-mode imaging and elastography, and vascular hemodynamics using Doppler imaging.⁷ The disadvantage for this imaging platform is that it is not applicable to study microvascular perfusion. In tandem with LSI, Doppler ultrasound may provide comprehensive information on wound tissue perfusion as well as changes in wound depth over time.

FUTURE PERSPECTIVES AND CONCLUSIONS

It is only a matter of time that imaging platforms will be an integral part of wound clinics. Based on the current state of hardware and software capabilities, it is predictable that most clinical systems will be turn-key. However, it would be necessary for clinical staff to train such that data collection may be conducted in a productive manner. It would also be important to recognize the specific advantages and limitations of each imaging platform such that data interpretation is well guided. The need to estimate wound depth is critical in both chronic wound and burn injury settings. The use of harmonic ultrasound technology for that purpose would be productive. Options for the study of tissue vascularization are many. If noncontact and noninvasive criteria are of importance, LSI is powerful. A major advantage of harmonic ultrasound imaging of wound depth is that the same system is capable of providing information on blood flow dynamics in gated feeder arteries or perforators. With many productive

imaging platforms to choose from, wound care is about to be transformed by technology that would help assess wound severity and estimate healing potential.

Chandan K. Sen, PhD

Center for Regenerative Medicine & Cell-Based Therapies
The Ohio State University Wexner Medical Center
473 West 12th Ave
Columbus, OH 43210
chandan.sen@osumc.edu

ACKNOWLEDGMENT

Work on wound closure and imaging in the authors' laboratory is supported by GM069589, GM077185, GM108014, NR013898, and NR015676.

REFERENCES

1. Brem H, Sheehan P, Rosenberg HJ, et al. Evidence-based protocol for diabetic foot ulcers. *Plast Reconstr Surg*. 2006;117:193S–209S.
2. Shupp JW, Nasabzadeh TJ, Rosenthal DS, et al. A review of the local pathophysiologic bases of burn wound progression. *J Burn Care Res*. 2010;31:849–873.
3. Kowalske KJ. Burn wound care. *Phys Med Rehabil Clin N Am*. 2011;22:213–227.
4. Jaskille AD, Ramella-Roman JC, Shupp JW, et al. Critical review of burn depth assessment techniques: part II. Review of laser Doppler technology. *J Burn Care Res*. 2010;31:151–157.
5. Jaskille AD, Shupp JW, Jordan MH, et al. Critical review of burn depth assessment techniques: Part I. Historical review. *J Burn Care Res*. 2009;30:937–947.
6. Monstrey S, Hoeksema H, Verbelen J, et al. Assessment of burn depth and burn wound healing potential. *Burns*. 2008;34:761–769.
7. Gnyawali SC, Barki KG, Mathew-Steiner SS, et al. High-resolution harmonics ultrasound imaging for non-invasive characterization of wound healing in a pre-clinical swine model. *PLoS One*. 2015;10:e0122327.
8. Langemo D, Anderson J, Hanson D, et al. Measuring wound length, width, and area: which technique? *Adv Skin Wound Care*. 2008;21:42–45; quiz 5–7.
9. White PJE, Podaima BW, Friesen MR. Algorithms for smartphone and tablet image analysis for healthcare applications. *Access, IEEE* 2014;2:831–840.
10. Poon TWK, Friesen MR. Algorithms for size and color detection of smartphone images of chronic wounds for healthcare applications. *Access, IEEE* 2015;3:1799–1808.
11. Kumar KS, Reddy BE. Digital analysis of changes in chronic wounds through image processing. *Int J Signal Process*. 2013;6:367–380.
12. Mukherjee R, Manohar DD, Das DK, et al. Automated tissue classification framework for reproducible chronic wound assessment. *Biomed Res Int*. 2014;2014:851582.
13. Bills JD, Berriman SJ, Noble DL, et al. Pilot study to evaluate a novel three-dimensional wound measurement device. *Int Wound J*. E-published ahead of print November 11, 2015.
14. Davis AJ, Nishimura J, Seton J, et al. Repeatability and clinical utility in stereophotogrammetric measurements of wounds. *J Wound Care*. 2013;22:90–2, 94.
15. Van Hecke LL, De Mil TA, Haspelslagh M, et al. Comparison of a new laser beam wound camera and a digital

- photoplanimetry-based method for wound measurement in horses. *Vet J*. 2015;203:309–314.
16. Lucas VS, Burk RS, Creehan S, et al. Utility of high-frequency ultrasound: moving beyond the surface to detect changes in skin integrity. *Plast Surg Nurs*. 2014;34:34–38.
 17. Goans RE, Cantrell JH Jr, Meyers FB. Ultrasonic pulse-echo determination of thermal injury in deep dermal burns. *Med Phys*. 1977;4:259–263.
 18. D'Astous FT, Foster FS. Frequency dependence of ultrasound attenuation and backscatter in breast tissue. *Ultrasound Med Biol*. 1986;12:795–808.
 19. Hoskins PR, Martin K, Thrush A. *Diagnostic Ultrasound: Physics and Equipment*. Cambridge: Cambridge University Press; 2010.
 20. Krouskop TA, Wheeler TM, Kallel F, et al. Elastic moduli of breast and prostate tissues under compression. *Ultrasound Imaging*. 1998;20:260–274.
 21. Coutts L, Bamber J, Miller N. Multi-directional *in vivo* tensile skin stiffness measurement for the design of a reproducible tensile strain elastography protocol. *Skin Res Technol*. 2013;19:e37–e44.
 22. Gennisson JL, Deffieux T, Fink M, et al. Ultrasound elastography: principles and techniques. *Diagn Interv Imaging*. 2013;94:487–495.
 23. F. UDoHaHS. *Guidance for Industry: Chronic Cutaneous Ulcer and Burn Wounds - Developing Products for Treatments*. Rockville, MD: Office of Training and Communication, Food and Drug Administration; 2006.
 24. Roy S, Elgharably H, Sinha M, et al. Mixed-species biofilm compromises wound healing by disrupting epidermal barrier function. *J Pathol*. 2014;233:331–343.
 25. Hudson TJ. Skin barrier function and allergic risk. *Nat Genet*. 2006;38:399–400.
 26. Ghatak S, Chan YC, Khanna S, et al. Barrier function of the repaired skin is disrupted following arrest of dicer in keratinocytes. *Mol Ther*. 2015;23:1201–1210.
 27. Kunii T, Hirao T, Kikuchi K, et al. Stratum corneum lipid profile and maturation pattern of corneocytes in the outermost layer of fresh scars: the presence of immature corneocytes plays a much more important role in the barrier dysfunction than do changes in intercellular lipids. *Br J Dermatol*. 2003;149:749–756.
 28. Segre JA. Epidermal barrier formation and recovery in skin disorders. *J Clin Invest*. 2006;116:1150–1158.
 29. Mustoe TA, Gurjala A. The role of the epidermis and the mechanism of action of occlusive dressings in scarring. *Wound Repair Regen*. 2011;19:s16–s21.
 30. Suetake T, Sasai S, Zhen YX, et al. Functional analyses of the stratum corneum in scars. Sequential studies after injury and comparison among keloids, hypertrophic scars, and atrophic scars. *Arch Dermatol*. 1996;132:1453–1458.
 31. Schäfer M, Werner S. Cancer as an overhealing wound: an old hypothesis revisited. *Nat Rev Mol Cell Biol*. 2008;9:628–638.
 32. Sinha M, Ghatak S, Roy S, et al. microRNA-200b as a switch for inducible adult angiogenesis. *Antioxid Redox Signal*. 2015;22:1257–1272.
 33. Bates DO, Harper SJ. Regulation of vascular permeability by vascular endothelial growth factors. *Vascul Pharmacol*. 2002;39:225–237.
 34. Dvorak HF. Vascular permeability factor/vascular endothelial growth factor: a critical cytokine in tumor angiogenesis and a potential target for diagnosis and therapy. *J Clin Oncol*. 2002;20:4368–4380.
 35. Demidova-Rice TN, Durham JT, Herman IM. Wound healing angiogenesis: innovations and challenges in acute and chronic wound healing. *Adv Wound Care (New Rochelle)*. 2012;1:17–22.
 36. Guo S, Dipietro LA. Factors affecting wound healing. *J Dent Res*. 2010;89:219–229.
 37. Sen CK. Wound healing essentials: let there be oxygen. *Wound Repair Regen*. 2009;17:1–18.
 38. Comerota AJ, Throm RC, Kelly P, et al. Tissue (muscle) oxygen saturation (StO₂): a new measure of symptomatic lower-extremity arterial disease. *J Vasc Surg*. 2003;38:724–729.
 39. Fife CE, Smart DR, Sheffield PJ, et al. Transcutaneous oximetry in clinical practice: consensus statements from an expert panel based on evidence. *Undersea Hyperb Med*. 2009;36:43–53.
 40. Lu G, Fei B. Medical hyperspectral imaging: a review. *J Biomed Optics*. 2014;19:010901–010923.
 41. Rossi A, Acito N, Diani M, et al. Hyperspectral data collection for the assessment of target detection algorithms: the Viareggio 2013 trial. In: *Proceedings of SPIE - The International Society for Optical Engineering 9250*. 2014. pp. 92500V-V-14.
 42. Chen PC, Lin WC. Spectral-profile-based algorithm for hemoglobin oxygen saturation determination from diffuse reflectance spectra. *Biomed Opt Express*. 2011;2:1082–1096.
 43. Gillies R, Freeman JE, Cancio LC, et al. Systemic effects of shock and resuscitation monitored by visible hyperspectral imaging. *Diabetes Technol Ther*. 2003;5:847–855.
 44. Greenman RL, Panasyuk S, Wang X, et al. Early changes in the skin microcirculation and muscle metabolism of the diabetic foot. *Lancet*. 2005;366:1711–1717.
 45. Xu RX, Allen DW, Huang J, et al. Developing digital tissue phantoms for hyperspectral imaging of ischemic wounds. *Biomed Opt Express*. 2012;3:1433–1445.
 46. Gurtner GC, Jones GE, Neligan PC, et al. Intraoperative laser angiography using the SPY system: review of the literature and recommendations for use. *Ann Surg Innov Res*. 2013;7:1.
 47. Alander JT, Kaartinen I, Laakso A, et al. A review of indocyanine green fluorescent imaging in surgery. *Int J Biomed Imaging*. 2012;2012:940585.
 48. Still JM, Law EJ, Klavuhn KG, et al. Diagnosis of burn depth using laser-induced indocyanine green fluorescence: a preliminary clinical trial. *Burns*. 2001;27:364–371.
 49. Deka G, Wu WW, Kao FJ. *In vivo* wound healing diagnosis with second harmonic and fluorescence lifetime imaging. *J Biomed Opt*. 2013;18:061222.
 50. Paul DW, Ghassemi P, Ramella-Roman JC, et al. Noninvasive imaging technologies for cutaneous wound assessment: a review. *Wound Repair Regen*. 2015;23:149–162.
 51. Sabapathy V, Mentam J, Jacob PM, et al. Noninvasive optical imaging and *in vivo* cell tracking of indocyanine green labeled human stem cells transplanted at superficial or in-depth tissue of SCID mice. *Stem Cells Int*. 2015;2015:606415.
 52. Atmaca LS, Sonmez PA. Fluorescein and indocyanine green angiography findings in Behçet's disease. *Br J Ophthalmol*. 2003;87:1466–1468.
 53. Stewart CJ, Gallant-Behm CL, Forrester K, et al. Kinetics of blood flow during healing of excisional full-thickness skin wounds in pigs as monitored by laser speckle perfusion imaging. *Skin Res Technol*. 2006;12:247–253.
 54. Roustit M, Cracowski JL. Assessment of endothelial and neurovascular function in human skin microcirculation. *Trends Pharmacol Sci*. 2013;34:373–384.
 55. Kilarski WW, Samolov B, Petersson L, et al. Biomechanical regulation of blood vessel growth during tissue vascularization. *Nat Med*. 2009;15:657–664.
 56. Klucinec B, Scheidler M, Denegar C, et al. Effectiveness of wound care products in the transmission of acoustic energy. *Phys Ther*. 2000;80:469–476.